Influence of spray impingement on gas surface heat transfer

Garbero M.[1], Fritsching U.[1], Vanni M.[2]

1. Verfahrenstechnik, Universität Bremen
Badgasteiner Straße 3, D-28359 Bremen – Germany.
2. Dip. Scienza dei Materiali e Ingegneria Chimica, Politecnico di Torino,
C.so Duca degli Abruzzi 24, 10129 Torino – Italy.

The paper analyses the behaviour of the heat transfer coefficient between air and a solid wall during drop impingement in a spray deposition process.
The air stream flow has been studied during the collision of a single droplet on a surface at different impact velocities for two different air flux configurations by means of the fluid dynamic code Fluent. A "Volume Of Fluid" model has been adopted for the determination of the shape of the gas-liquid interface.
The work shows that the droplet influences remarkably the air flow fluid and the temperature profiles close to the surface. The droplet, approaching the surface, establishes a circulation of air near the wall that increases surface heat transfer considerably.
A simple analysis has been also done in the case of multiple impacts. Here the results evidence further the great influence of droplet wakes on temperature and velocity profiles.
The change in the gas velocity and temperature distribution due to the two phase flow has been investigated by Euler-Lagrange simulations as well. It has been shown that the prediction of the heat transfer coefficient obtained by standard wall treatment can be inaccurate, because of its inability to describe in detail the surface layer.

1. Introduction

The study of thermal effects related to spray impingement on solid walls has attracted recently much attention, connected to the development of new processes as spray forming, to spray painting applications and to metallization coatings for microelectronics components. The physical phenomena controlling the deposition process are of great importance for the improvement of all these applications. Here a huge amount of strictly connected parameters has to be analysed in order to optimise structure, characteristics and resistance qualities of the sprayed product.
In order to achieve accurate prediction of the resulting deposit morphology and microstructure, it is essential to understand the fluid dynamics of the droplets during both their flying towards the surface and their impact phase, as well as mass and heat transfer between drop, air and surface.
One important parameter is the heat transfer coefficient between gas and solid surface. So far little attention has been paid to gas-surface heat transfer [1-2], since it is well known that the corresponding coefficient is typically several orders of magnitude smaller than the heat transfer coefficient between droplet and surface [3-4]. Nevertheless, in a number of

applications droplets and surface have very close temperatures: in these cases gas-solid heat transfer becomes comparable to that between impacting droplets and surface and thus it may determine the processes of solidification or levelling that follow the impingement phase.
The dynamics of the heat transfer during spray impact has been analysed both from a micro- and a macro-scale point of view.
The micro-scale analysis investigates the disturbances originated by a droplet on the gas temperature and velocity profiles at the scale of the droplet. A fully developed boundary layer profile has been assumed as the undisturbed gas condition and the liquid spread on to a smooth surface has been simulated for single and multiple impacts and for different droplet and gas velocities.
The interaction between droplet and rigid walls is rather complex, because of the large number of influencing factors. The outcome of the impingement of an individual droplet may be its deposition on the surface (spreading) or its re-atomisation into smaller secondary droplets with partial mass deposition (splashing). Of course spreading is the desired condition in spray deposition processes and therefore it has been assumed in our simulations. Its actual occurrence in the studied conditions has been verified by applying the criteria proposed by the groups of Mundo and Bussmann [5-6].
The spreading of a droplet is always followed by its partial recoiling, which is driven by surface tension. A further analysis has shown that in the our case the extent of recoiling is negligible, due to the high viscosity and to the small surface tension of the liquid adopted in the simulations. The high viscosity dissipates rapidly the inertia of the droplet and the small surface tension does not provide enough elastic energy to retract the lamella [7]. Furthermore such a behaviour makes it possible to adopt a constant value for the solid-liquid contact angle, without considering different values for the advancing and receding liquid front. In this work, a static contact angle of 90° has been assumed.
On the macro-scale, the interaction between particle trajectories and gas flow has been simulated for an impinging jet. Here the heat transfer coefficient has been calculated with and without particles for different downloading values.

2. Analysis of the impact

2.1. Method of simulation

The fall of the droplets and their spread on to a smooth surface have been simulated by means of the VOF model [8-9]. Here a single momentum equation is solved throughout the domain and the resulting velocity field is shared among the phases.
The flow has been modelled as laminar, since only a thin layer of gas, very close to the solid surface, has been considered. In order to track the gas-liquid interface a continuity equation for the volume fraction of the liquid is solved connected to the geometric reconstruction scheme. This piecewise-linear approach calculates the position and the orientation of the linear interface relative to the centre of each partially-filled cell of the computational domain, based on information about the liquid volume fraction and its derivatives in the cells. The effect of surface tension has been included by means of the Continuous Surface Model proposed by Brackbill *et al.* [10].
In this model surface tension acts as a body force over the region in which the volume fraction of liquid varies, while the prescription on the contact angle results in an adjustment of the curvature of the surface near the wall.

In order to compute the heat transfer flux between gas and surface, the total enthalpy equation from the energy balance shared among liquid and gas can be solved:

$$\frac{\partial}{\partial t}(\rho H) + \nabla \cdot (\rho \vec{u} H) = \nabla \cdot \left(\frac{k}{c_p} \nabla H \right) \tag{1}$$

The conduction and the species diffusion terms combine to give the first term on the right hand side of the above equation. The total enthalpy H is defined as:

$$H = \sum_i y_i H_i \tag{2}$$

Where y_i is the mass fraction of the single phase i and $H_i = \int_{T_{ref,i}}^{T} c_{p,i} dT + h_i^0(T_{ref,i})$.

$h_i^0(T_{ref,i})$ is the formation enthalpy of species i at the reference temperature $T_{ref,i}$.
Neglecting the heat flux due to species diffusion and considering the specific heat capacity c_p independent by temperature, equation (1) can be written only in term of temperature:

$$\rho c_p \frac{\partial T}{\partial t} + \rho c_p \nabla \cdot (\vec{u} T) = \nabla \cdot (k \nabla T) \tag{3}$$

where the values of k, ρ, c_p depend on the local liquid volume fraction α; for instance $k = \alpha k_l + (1- \alpha) k_v$. From Equation (1) the temperature field can be obtained in the entire computational domain. Being the gas flow laminar, the heat transfer coefficient can be computed using Fourier's law applied to the wall:

$$h = \frac{-k\left(\frac{\partial T}{\partial n}\right)}{T_w - T_f} \tag{4}$$

and the heat flux to the wall from a fluid cell can be find as $Q = h\,(T_w - T_f)$.

2.2. Impact of a single droplet

In order to simulate the interaction between droplets and gas flow, the velocity and temperature profiles occurring in a boundary layer flow over a flat plate at a distance of 10 cm from the beginning of the plate have been used as the undisturbed flow and thermal fields. Two cases have been considered, with free stream velocity U of 20 and 40 m/s, respectively. For these conditions the Reynolds gas number is $1.38 \cdot 10^5$ and $2.75 \cdot 10^5$; both values are below the laminar-turbulent transition of $5 \cdot 10^5$, thus indicating a laminar situation. The domain is 2 mm width, 0.8 mm deep and 1.5 mm high and is composed by 300˙000 cubic cells with edge of 20 μm. The height of the undisturbed velocity boundary layer profile is 1.35 mm in one case and 0.95 mm in the other one. The height of the temperature profile is slightly larger, because Prandtl number for the gas phase is 0.713, but still lower than the height of the considered domain in both test cases. The maximum temperature difference in the test cases has been of 20 K. The droplets are inserted in the computational domain at a distance H of 1.1 mm from the surface and X = 0.5 mm from the gas inlet section (as shown

in Fig. 1). They have a diameter D of 200 μm and initial velocity U_p of 5, 10, or 20 m/s in the direction perpendicular to the solid surface. In this conditions the values of drop Reynolds numbers are 27, 53 and 106, while whose of Weber numbers are 177, 709 and 2˙835, respectively. A time step of 10^{-8} s has been adopted in all the test cases to ensure accuracy. Such a small step is required because of the large velocity difference between gas and droplet that may reduce the quality of the prediction near the interface. For better estimation of the heat transfer coefficient, the liquid surface after drop spreading has been considered as part of the total heat exchange surface.

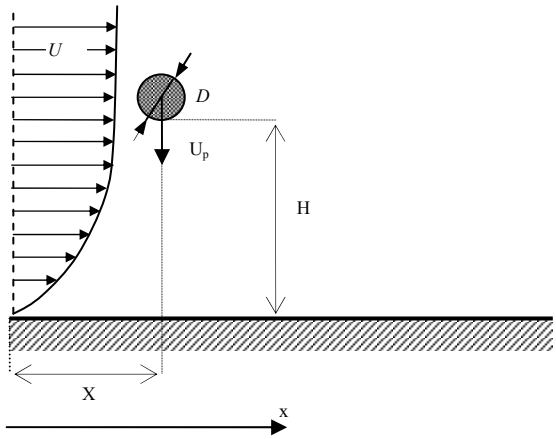

Fig. 1. Representation of the initial condition for the impact of a single droplet.

Fig. 2 shows the increase of the instantaneous Nusselt number (averaged over the considered wall surface of 1.6 mm^2) just before drop impact as a function of dimensionless time. The increase of heat transfer depends above all by the difference of velocity magnitude between gas and droplet. The drop here acts like an obstacle to overpass for the gas flow: if it falls down quickly, the gas flow underneath the droplet is more cut than disturbed and, as a consequence, there is only a narrow heat flux increment. On the contrary, at lower drop velocities, where a larger amount of air can flow under the drop, the gas stream is more compressed and the temperature gradient becomes larger. For the same difference of velocity magnitude, the increase of heat flux is remarkably larger in the case of higher gas velocities. The curves show a maximum immediately before the collision between droplet and surface, that takes place at τ=0 in the diagram.

Fig. 3 reports the variation of the Nusselt number after impact. The diagram shows a much larger increment in heat flux in comparison to Fig. 2, both in magnitude and in duration, due to the stronger drop influence on velocity and temperature profile after impact.

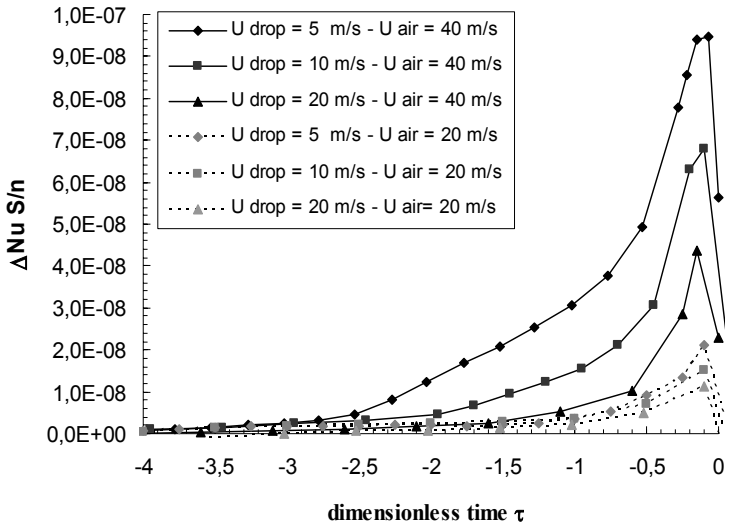

Fig. 2. Variation of the average surface Nusselt number before impact. Drop diameter: 200 μm.

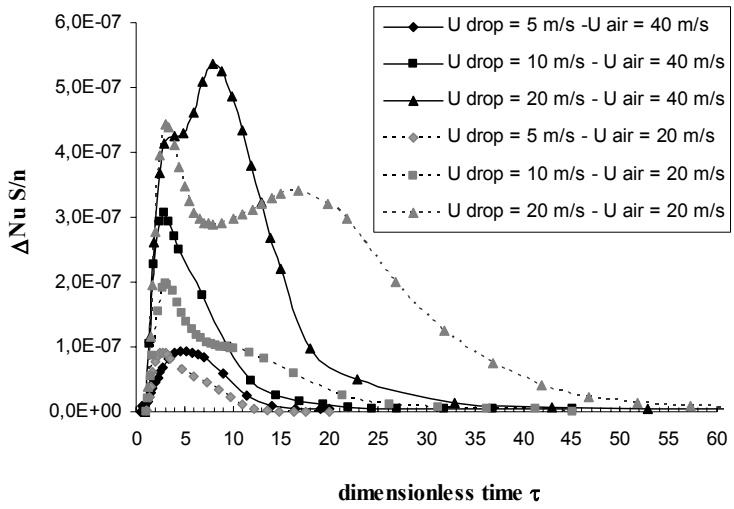

Fig. 3. Variation of the average surface Nusselt number after impact. Drop diameter: 200 μm.

The falling drop leaves a wake on its backside, which persists for some time even after the impact (see Fig. 4 (a)). The air in this wake, dragged by the droplet, is cooler than the air near the surface and increases heat transfer significantly. The mechanism is confirmed by Fig. 4 (b): the local increment of the heat transfer reaches a very high value immediately after the spread, when the fresh air of the wake reaches the surface. Subsequently the low temperature region expands on the surface on the influence of the main gas flow field. Due to this reason, the curves, of Fig. 3, at the highest impact velocity show a bimodal effect. The first maximum is due to a peak in the local heat transfer, meanwhile the second one is the result of a smaller heat flux increment spread on a larger part of the surface. Apart from the case with impact velocity of 10 m/s and air velocity of 40 m/s, where the two effects happen at the same time, the increment of Nusselt in the first part of the curve is directly proportional to $Re_p^{-1,13}$.

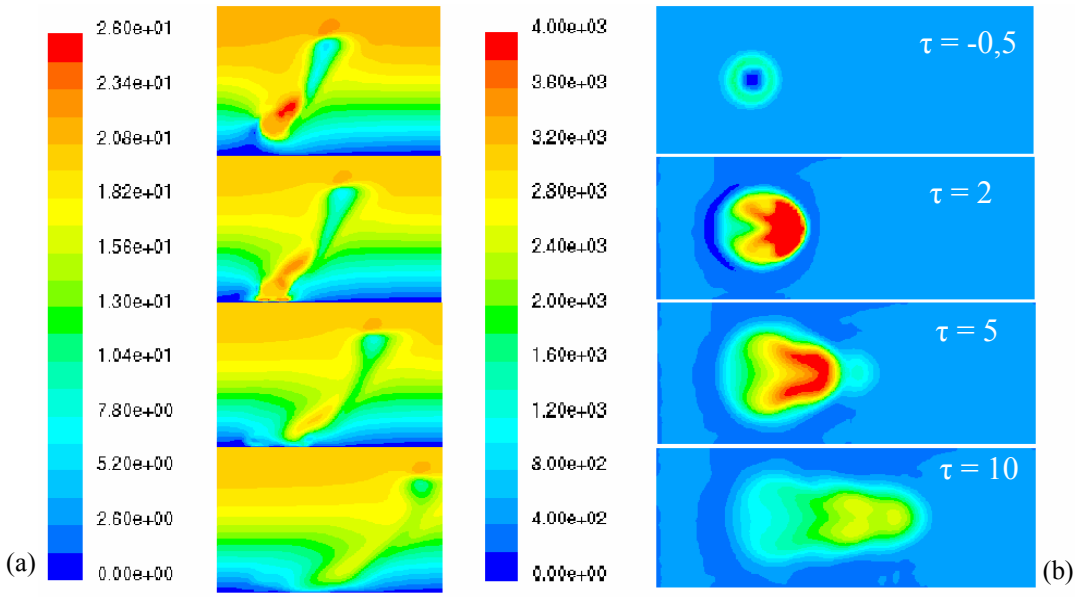

Fig. 4. (a) Contours of velocity magnitude [m/s] and (b) contours of total surface heat flux [w/m^2]. Droplet diameter: 200 μm, droplet velocity: 10 m/s, maximum gas stream velocity: 20 m/s.

The different duration of the phenomenon can be explained by considering the role of the wake. For high difference of velocities between gas and drop, the wake of the droplet is blown by the air flow behind the droplet in a horizontal direction, meanwhile for small difference of velocities the wake follows the droplet along the vertical direction of impact. In this case, since the wake is aligned nearly vertically, the increase of heat transfer lasts for a longer time. On the contrary, at small impact velocity, the interaction between drop and gas reduces the wake practically to a stagnation zone in the region not directly exposed to the gas flow. Also here some cool gas can reach the surface, but in a lower quantity and for a smaller time.
To be noted is the case regarding the smallest impact velocity and the maximum gas flow velocity. Here the stagnation zone interacts with the air compressed by the droplet before impact forming a stagnant gas layer on the surface. As a consequence the gas flow takes more time to blow away the cooler air entrapped in the wake and to reduce the increase of the heat flux. This is showed well in Fig. 3, where the curve regarding the impact velocity of 5 m/s and the air velocity of 40 m/s has the slowest behaviour compared to all the others curves.

2.3. Impact of multiple droplets

So far, attention has been focussed on the study of the single drop case, but real sprays are composed by swarms of droplets. For example, considering a spray process with a liquid mass flow rate of 0.1 kg/s, at a distance of 50 cm from the nozzle, a typical figure for the number of particles that impact the wall per unit time is $3 \cdot 10^9$ $m^{-2}s^{-1}$, that means one impact every 0.2 ms on the considered surface of 1.6 mm^2. If the interaction among particles is neglected, one can argue that every drop adds its contribution ΔQ to the global heat transferred from gas to solid. Therefore, by time averaging the Nusselt number over a cycle of 0.2 ms, the effective heat transfer coefficient can be calculated. For example analysing the case of drop impact velocity of 10 m/s and maximum gas velocity of 20 m/s, the effective heat transfer coefficient evaluated by this procedure is 43 W/m^2K, a value sensibly higher than that without droplets: 27 W/m^2K, showing that the effect of droplets on gas-solid heat transfer is significant. Of course the method should be regarded as an approximation, valid for very dilute sprays only. In fact, proceeding in such a way, we do not consider the interaction among the wakes behind droplets, which can change dramatically the increase of heat transfer with respect to the situation computed as before. This is especially true at high concentration when the distance between particles is small.
In order to study this interaction, two cases have been considered: with 3 and 5 droplets in the computational domain and an impact velocity of 10 m/s. Periodic boundary conditions have been used for gas inlet and exit sections; as before the undisturbed gas flow and thermal fields is that of a boundary layer with free stream velocity of 20 m/s. The distance between the centres of the droplets is of 0.72 mm in the former case and of 0.78 mm in the latter. Before impact, every droplet makes heat transfer increase in the same way as seen before for the case of a single drop. The main difference appears when the last droplets are approaching the surface, since they do not move in an undisturbed boundary layer profile, but interact with the wakes of the previous droplets.
If the new approaching droplet collides the surface in the same position as the previous drop, normally it helps the gas dragged by the former droplet to spread on the surface, increasing heat transfer considerably; on the contrary if the drop does not collide the surface in the same position, it may even reduce the circulation of gas, thus resulting in a smaller increment of heat transfer.

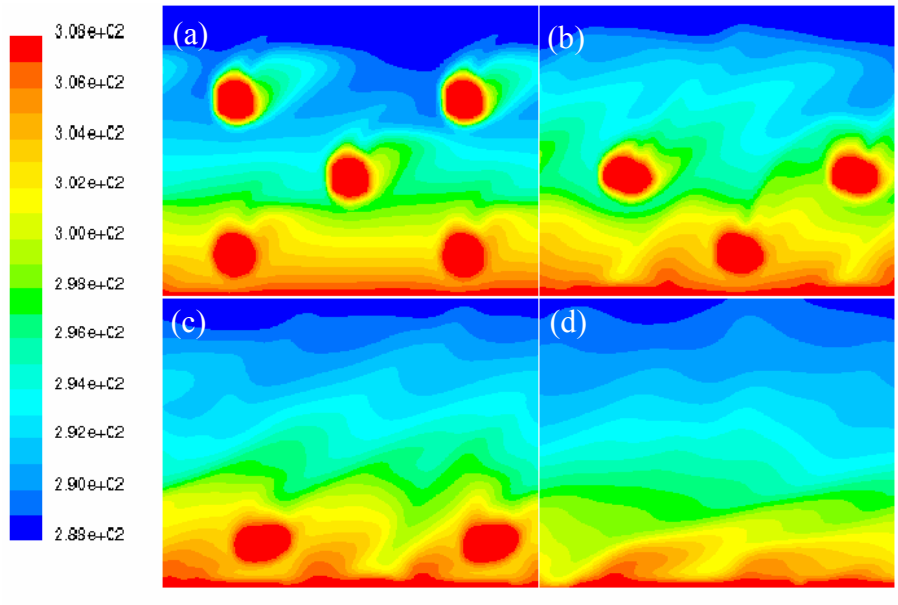

Fig. 5. Temperature contours T=[K], during 5 droplets impact: droplet diameter 200 μm, droplet velocity: 10 m/s, maximum gas velocity: 20 m/s. (a) 0 s, (b) 0,04 ms, (c) 0,08 ms (d) 0,2 ms

The effect is apparent in Fig. 5, where the temperature fields at different times are reported for the case of 5 droplets. In the first frame the first two droplets are on the point of colliding the surface. The gas flow is compressed by droplets and bends over them. As a consequence locally velocity and temperature gradients are higher and the heat flux increases.
In frame (b) two zones of low temperature just above the previously spread droplets show the cold gas reaching the surface. Here a third drop begins to influence the gas flow below it, but acts as an obstacle for the circulation of the warm gas established by the first drop on its left, reducing the locally heat flux transfer.
When the last two droplets arrive close to the surface, the zones with small temperature are compressed between drop and wall and a larger gas circulation is achieved. After that the gas dragged by the last two droplets interacts with the circulation phenomena established by the other droplets, before achieving the unperturbed condition under the influence of the boundary gas flow.

3. The impinging jet

3.1. Modelling

For the macroscopic simulation of the impinging jet the Euler-Lagrange approach implemented in the CFD code Fluent has been adopted. The prediction of the gas flow is obtained by solving the averaged Navier-Stokes equation in connection with the RNG k-ε model for turbulence [11-12]. For accurate prediction of velocity and thermal profiles near the wall, a wall treatment method that combines a two-layer model [13] with enhanced wall functions [14] has been used.
The dispersed phase is treated by the Lagrangian approach. Here a large number of droplet parcels, representing a certain amount of real droplets with the same properties, are traced through the flow field. The representation of droplets by parcels makes it possible to consider size distribution and to simulate the measured liquid mass flow rate at the injection locations

by a reasonable number of computational droplets. The trajectory of each droplet parcel is calculated solving the equation of motion for a single droplet, taking into account the drag between particles and the gas phase [15]. The drag coefficient C_D has been calculated from the following equation [16]:

$$C_D = \frac{24}{\mathrm{Re}}\left(1 + 0.15\,\mathrm{Re}_p^{0.687}\right) \qquad \mathrm{Re}_p < 500 \tag{5}$$

In order to model the droplet dispersion in turbulent flow and to obtain a representation of the local velocity, the eddy lifetime concept can be applied [17]. This model assumes that the droplet interacts with a sequence of turbulent eddied with randomly sampled fluctuations.
The calculation of the temperature field has been made by means of the energy balance. In this equation an additional source term taking into account viscous dissipation, which describe the thermal energy created by viscous shear in the gas flow, has been considered. To estimate wall heat transfer the Reynolds analogy between momentum and energy transport has been applied. In such a way a thermal conduction sublayer and a region where turbulence effects prevail have been coupled to describe the temperature profile. An effective conductivity (turbulent plus molecular) was used to obtain the heat transfer coefficient at the wall.

3.2. Results

An air stream flow, exiting a circular nozzle (see Fig. 6) of 1 cm diameter D with an average velocity U of 20 m/s and cooling a flat surface at a distance H = 10 cm far from the nozzle has been considered. The difference in temperature between air and surface has been set at 20 K. The integral averaged Nusselt number at different values of radius has been calculated for the case of an air stream without particles and for two different values of spray loading, corresponding to mass download values W of 1 and 2, respectively. A particle injection with a Rosin Rammler size distribution and a mean particle diameter of 100 μm has been used as source terms for droplets. The injection has been located at the nozzle exit with a velocity of 20 m/s in the wall direction. In order to verify the profiles of mean velocity and temperature predicted by the CFD code, a comparison with the correlation of Schlünder und Gnielinski [18] has been done for the case without droplet. Fig. 7 shows the good agreement between simulations and correlation and the increase of the Nusselt number due to particle flow. The curves have a maximum in correspondence of the centre of the spray. Here the gas flow strongly deviates, turbulence is more intense and the temperature gradients are higher. Introducing the particles, the inertia of droplets affects the gas flow increasing the heat flux. The effect of particle is restricted to a small area with a radius of 1 cm near the core of the spray where the droplet impacts the surface. In the remaining part of the surface there are no droplets since a condition of trap at the wall has been considered and the heat transfer does not change.

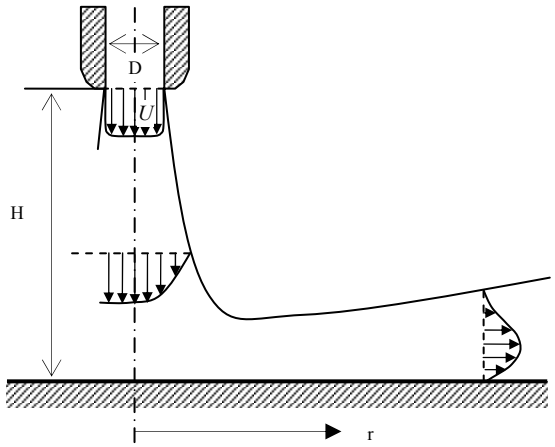

Fig. 6. The impinging jet.

In order to evidence one more time the importance of studying also spray on a micro scale, the overall heat transfer coefficient found by Euler-Lagrange simulations has been compared with the experiments of Yokomine *et al.* [1]. When the droplet do not rebound on the surface, it appears that the theoretical Nusselt number is sensibly smaller that the corresponding one achieved by experiments. Obviously, This is due to the fact that the Euler-Lagrange approach consider volumeless particles and thus it cannot model in detail the droplet-surface-gas interaction that originates the increase of heat transfer.

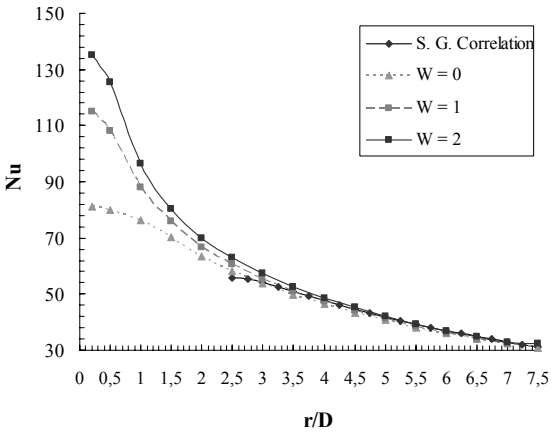

Fig. 7. Integral average of Nusselt number in function of dimensionless radius.

4. Conclusions

In this paper the influence of spray impingement on gas surface heat transfer has been analyzed both from a micro and a macro scale point of view. On micro scale the fluid dynamics influence of drop impingement within a laminar boundary layer has been simulated by means of a VOF technique. It has been shown that the droplets that are approaching the surface act as eddy generators, establishing a circulation of air near the wall that can increase surface heat transfer considerably.
On a macro scale a two-phase jet impingement case has been studied by means of an Euler-Lagrange approach. Here, droplets affect the gas flow giving larger inertia. The larger inertia creates higher velocity near the wall increasing the temperature gradients. Nevertheless, the larger influence seems to be near the wall in the laminar layer. Here the laminar layer at the wall is strongly perturbed and the standard wall treatment should be corrected in the prediction of the heat transfer exchange at the wall.

5. Nomenclature

μ	viscosity	S	impact surface
C_D	drag coefficient	t	time
c_p	specific heat capacity	T	temperature
D	droplet diameter before impact	T_w	wall temperature
h	heat transfer coefficient	$\vec{u}$	gas velocity (vector)
H	total enthalpy	U	magnitude gas velocity (scalar)
k	conductivity	U_p	droplet velocity before impact
n	number of droplets	W	mass downloading
Nu	Nusselt number, hD/k	We	Weber number, $\rho DU_p^{\,2}/\sigma$
Q	heat flux	y	liquid mass fraction
r	impact surface radius	ρ	density
Re	gas Reynolds number, $\rho DU/\mu$	τ	dimensionless time, tU_p/D
Re_p	particle Reynolds number, $\rho DU_p/\mu$	σ	surface tension

6. Reference

[1] Yokomine T, Shimizu A, Saitoh A and Higa K 2002 *Exp. Therm. Fluid Sci.* **26** 617-626
[2] Sun J and Chen M M 1998 *Int. Heat Mass Trasfer* **31** 969-975
[3] Armster S A, Delplanque J P, Rein M and Lavernia E J 2002 *Int. Mat. Rev.* **47** 265-300
[4] Pasandideh-Fard M, Chandra S and Mostaghimi J 2002 *Int. J. Heat Mass Transfer* **45** 2229-2242
[5] Mundo C, Sommerfeld M and Tropea C 1998 *Atomization and Sprays* **8** 625-652
[6] Bussmann M, Mostaghimi J and Chandra S 2000 *Phys. Fluids* **12** 3121-3132
[7] Garbero M, Vanni M and Baldi G 2002 *18th ILASS Conference* Zaragoza-Spain 123-128
[8] Kothe D B, Mjolsness R C and Torrey M D 1991 *Technical Report LA-12007-MS* LANL Los Alamos NM
[9] Hirt C W and Nichols B D 1981 *J. Comput. Phys.* **39**, 201-225
[10] Brackbill J U, Kothe D B and Zemach C 1992 *J. Comput. Phys* **100** 335-354
[11] Launder B E and Spalding D B 1972 *Lectures in Mathematical Models of Turbulence* (London Academic Press)
[12] Yakhot V and Orszag A 1986 *Journal of Scientific Computing* **1** 1-51
[13] Chan H C and Patel V C 1988 *AISS Journal* **26** 641-648
[14] Kader B 1993 *Int. J. Heat Mass Transfer* **24** 1541-1544
[15] Rüger M, Hohmann S, Sommerfeld M and Kohnen G 2000 *Atomization and Sprays* **10** 47-81
[16] Leger L, and Joanny J F 1992 J F *Rep. Prog. Rhys.* **55** 431-486
[17] Clift R and Gauvin W H 1970 Chemeca **70** 14-28
[18] Martin H 2002 *VDI Wärmeatlas* (Springer Berlin) **9** Gk1-Gk6